# Unified Feature Scale Model for Etching in $SF_6$ and Cl Plasma Chemistries

Xaver Klemenschits, Siegfried Selberherr, and Lado Filipovic
Institute for Microelectronics, TU Wien
Gußhausstraße 27-29/E360, 1040 Vienna, Austria
Email: klemenschits@iue.tuwien.ac.at

***Abstract*—A novel unified feature-scale model for inductive plasma etching is presented. The semi-empirical model simplifies simulations by considering only surface reactions and ignoring those in the reactor. The model gives an accurate description of passivation layers which form on sidewalls during etch processes, by treating them as independent materials. This allows them to be explicitly included in subsequent etch steps, resulting in a more accurate description of the physical process. Therefore, novel gate stack geometries for advanced nodes can be modelled more rigorously, enabling a better understanding of the complex chemical and physical processes taking place during the gate stack etching sequence. The model was applied in the analysis of a gate stack geometry for CMOS devices of a 14nm process and compared to experimental results, which are in good agreement.**

## I. Introduction

Over the past decades, microelectronic device dimensions have been decreasing, overcoming increasingly challenging lithography and fabrication limitations. Complex production techniques have been developed to meet the dimension requirements given in the ITRS roadmap [1]. Transistor high-k gate stack patterning is currently one of the greatest challenges in advanced-node fabrication. The complex, layered gates incorporate several materials, which all need a carefully controlled etching sequence. Even a single layer in a gate requires multiple etch steps, involving different chemistries, in order to achieve fine control over the details of the resulting geometry, such as sidewall tapering [2]. Many of these etch steps include the simultaneous deposition of polymers on the sidewalls and ion enhanced directional etching elsewhere, to achieve straight etch profiles. These polymers form a passivation layer, which will protect the underlying material in subsequent etch steps, preserving the tapered sidewalls. We propose a unified feature scale model for the simulation of such complex etch processes used in modern gate stack patterning, where the 14FDSOI [3] process serves as an appropriate example. The model was implemented in ViennaTS [4], a topography simulation tool employing levelset representations of surfaces, thereby enabling the unified simulation of intricate microelectronic process flows. Different materials can be modelled independently and accurately in order to understand the interactions between materials, which is especially important for characterising the behaviour of thin passivation layers and their effect on the subsequent etch steps and thus the final geometry.

## II. Unified Feature Scale Model

The proposed model assumes a steady-state flux impinging on the surface, which can be retrieved from experiments or chemical kinetic simulations. The chemical reactions, which depend on the gas chamber setup, take place in the reactor scale and ultimately generate the surface fluxes used in the feature-scale model. The chamber simulations required to generate the surfaces fluxes are beyond the scope of this work. The underlying assumption of the described model is that any complex plasma etch process involves the interaction of three types of particles: etchant, polymer depositing particles, and ions [5]. After introducing them into the reactor, each of these particles will react or absorb, at different rates, with the surface and effectively cover it. The respective surface coverages will depend on the surface geometry as well as the emission distribution of the particles. Although accelerated ions will not necessarily adsorb on the surface, the calculated coverage can be used as the rate of ion impact per unit time on the surface. Since the time scale of etch processes is much greater than that of surface reactions, the coverages can be assumed to reach a steady-state on the surface. Therefore, the surface coverages of all involved particle types $\phi_x$, where x represents etchant (e), polymer (p), etchant on polymer (pe), and ions (i), are expressed by the following steady-state equations:

$$\frac{d\phi_e}{dt} = J_e S_e (1 - \phi_e - \phi_p) - k_{ie} J_e \phi_e - k_{ev} J_{ev} \phi_e \approx 0 \quad (1)$$

$$\frac{d\phi_p}{dt} = J_p S_p - J_i Y_p \phi_p \phi_{pe} \approx 0 \quad (2)$$

$$\frac{d\phi_{pe}}{dt} = J_e S_{pe} (1 - \phi_{pe}) - J_i Y_p \phi_{pe} \approx 0 \quad (3)$$

$J_x$ and $S_x$ are the fluxes and sticking probabilities of the respective particle types. The variables $Y_x$ represent the ion-enhanced etching yields for polymer ($Y_p$), etchant ($Y_e$), and the sputtering yield ($Y_s$), while $k_x$ describe stoichiometric factors for ion-enhanced etching ($k_{ie}$) and evaporation ($k_{ev}$). The coverages of every point on the surface can be found by solving Eqs. (1) to (3). From these coverages the rate at which the surfaces grows (deposition) or decays (etching) can be found. If deposition dominates, the rate of growth is given by Eq. (4)

$$v = \frac{1}{\rho_d} \left( Y_p J_i \phi_{pe} - J_p S_p \right) \quad (4)$$

978-1-5386-4811-7/18/$31.00 ©2018 IEEE

The new material growing on top of the surface is represented as an independent levelset enabling the individual and simultaneous treatment of several materials on the surface. The deposition or etching of this new levelset follows the same equations, but using different parameter values since it describes a new material with etchant coverage given by $\phi_{pe}$. If etching dominates on the surface of the substrate, the following etch rate is applied to the top most material:

$$v = \frac{1}{\rho_m}\left(J_i Y_e \phi_e + J_i Y_s (1-\phi_e) + J_{ev}\phi_e\right) \tag{5}$$

The growth and etch rates depend on the densities of the polymer ($\rho_d$), in the case of deposition, and of the material being etched ($\rho_m$), in the case of etching. Adjusting the coefficients of Eq. (4) and Eq. (5) systematically, one can create a specific set, describing the overall behaviour of dry plasma etch techniques using a single unified modelling approach. The use of the levelsets, which implicitly define all surfaces, enables the accurate simulation of complex deformation, separation, and merger of surfaces, essential to properly treat the thin passivation layers, an important part of modern gate stack etching techniques. This is possible because ViennaTS allows for appropriate handling of material layers with thicknesses below a single grid unit. Therefore, this robust modelling enables the accurate simulation of complex processes, including material specific characteristics at any point in time. Since the deposited materials are tracked separately, they can be used in subsequent etch steps with different chemistries, allowing for an accurate description of complex fabrication techniques, even when dealing with several stacked thin layers. However, the proposed model treats interfaces between materials as sharp, abrupt changes in composition, which is not usually the case for materials at nanometre scales. Therefore, the material boundaries given by our simulations should not always be interpreted as strict edges, but they serve as guides indicating the relative concentrations of different materials at the interface.

## III. Implemented Chemical Models

A modern gate stack etching process, 14FDSOI, for the 14nm node [3] was chosen to demonstrate the versatility and robustness of the proposed model and its capability of describing complex etch processes accurately. The process consists of 5 etch steps: Poly-Silicon (Poly-Si) main etch ($SF_6$), Poly-Si over etch ($HBr/O_2$), Titanium Nitride (TiN) main etch ($Cl_2/CH_4$), TiN over etch ($Cl_2$) and Hafnium Silicon Oxide (HfSiO) etching ($BCl_3$). Each of these steps is carried out using different etch chemistries, making use of their individual properties to create straight profiles with accurate control over dimensions, both vertically and laterally. For each of these etch steps, the model parameters described earlier must be calibrated for an accurate behavioural representation over a wide range of values for each input parameter, such as impinging fluxes or reactor temperature and pressure. The presented models were calibrated using experimental results for each etch process in order to resemble experimental profiles as closely as possible.

### A. Etching in $SF_6$ Plasma

Sulphur Hexafluoride ($SF_6$) chemistries are usually used to etch Si and $SiO_2$ [6]. Due to the high volatility of the involved elements, many reactions take place on top of the etched surface. Simulating the discrete reactions is computationally expensive and might, in some cases, even be impossible, while the proposed semi-empirical approach provides a computationally cheaper alternative and delivers reliable results [7]. The described etching process builds passivation layers by forming a uniform polymer layer on top of the substrate, which is sputtered by incoming ions, leaving the polymer only on the vertical sidewalls by line of sight deposition. ViennaTS is able to provide this functionality, but since experiments show that this mechanism results in very thin, uniform passivation layers, it was incorporated into the model as a direct polymer deposition for higher computational efficiency, since the etched geometries were not complex enough to show strong shadowing effects. Fig. 1 shows the resulting geometries when using different etchant fluxes, demonstrating that the polymer on the trench sidewalls shields the bottom from the incoming etchant, creating high gradients in etchant concentration, which leads to a spear-shaped profile. For smaller etchant fluxes, this gradient is not as high, since different etch mechanisms dominate.

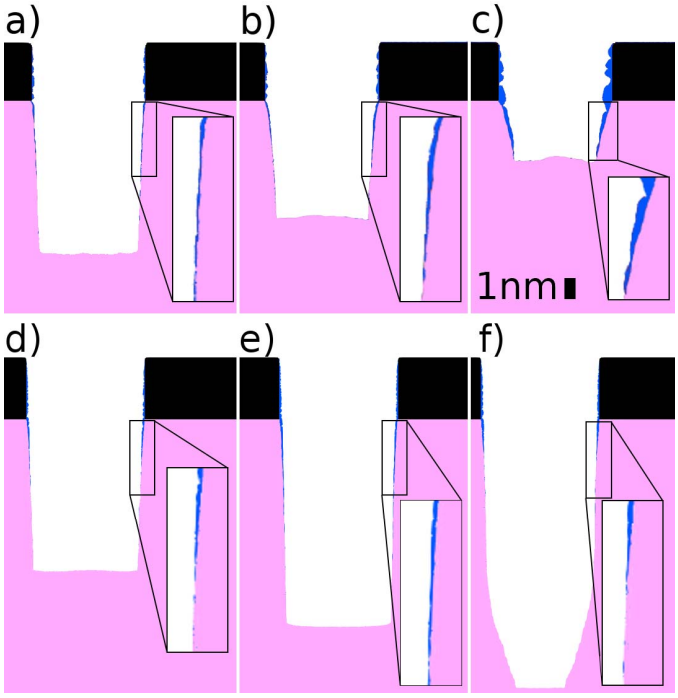


Fig. 1. Two-dimensional trenches formed by etching Silicon (pink) with a mask (black). The ion flux was kept constant at $10^{16}cm^{-2}s^{-1}$. In a)-c), the trenches were etched for 25s with a constant etchant flux of $1.3x10^{16}cm^{-2}s^{-1}$, while the polymer (blue) concentration was varied: a)$5x10^{15}cm^{-2}s^{-1}$, b)$10^{16}cm^{-2}s^{-1}$, and c) $5x10^{16}$ $cm^{-2}s^{-1}$. In d)-f), the polymer flux was constant at $5x10^{15}cm^{-2}s^{-1}$ and the etchant flux was changed: d)$5x10^{15}cm^{-2}s^{-1}$, e)$2x10^{16}cm^{-2}s^{-1}$, and f) $5x10^{16}$ $cm^{-2}s^{-1}$.

### B. Etching in $HBr/O_2$ Plasma

The hydrogen bromide etch process is used for its increased selectivity towards TiN, which lies underneath the Poly-Si. A thick passivation layer is formed by this etch chemistry on all Poly-Si surfaces, while ion-enhanced etching dominates the removal of Si [8]. This etch process is expected to give reliable results, even in complex geometries, as the passivation layers are formed purely chemically. Fig. 2 shows how this etch chemistry behaves for different etchant and polymer fluxes. The strong sensitivity to a change in polymer flux can be seen clearly in Fig. 2 a)-c), resulting in thicker passivation layers. Furthermore, in contrast to $SF_6$ etching, very high polymer fluxes result in thick passivation layers without a significant reduction in the etch rate.

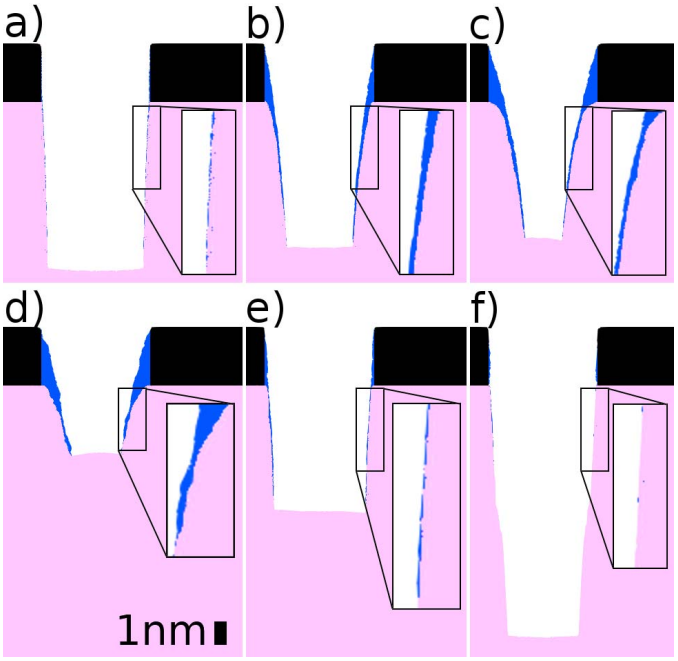


Fig. 2. $HBr/O_2$ etching of Silicon (pink) with a mask (black) for 25s. The ion flux was kept constant at $10^{16}cm^{-2}s^{-1}$. In a)-c), the Si was etched with a constant etchant flux of $1.0x10^{16}cm^{-2}s^{-1}$, while the polymer (blue) concentration was varied: a)$1x10^{16}cm^{-2}s^{-1}$, b)$3x10^{16}cm^{-2}s^{-1}$, and c) $5x10^{16}$ $cm^{-2}s^{-1}$. In d)-f), the polymer flux was constant at $1.0x10^{16}cm^{-2}s^{-1}$ and the etchant flux was changed: d)$1x10^{15}cm^{-2}s^{-1}$, e)$5x10^{15}cm^{-2}s^{-1}$, and f) $5x10^{16}$ $cm^{-2}s^{-1}$.

### C. Etching in $Cl_2/CH_4$ Plasma

Chlorine etching with $CH_4$ is used to etch TiN and forms thin amorphous passivation layers on TiN as well as Si. However, it is far less directional, with a lateral to vertical etch ratio of about 0.4, which creates the under-etch in the TiN layer seen in Fig. 3 [9]. The passivation layer is not visible due to the small amount of polymer present on the surface.

### D. Wet Etching with $Cl_2$ and $BCl_3$

The TiN over-etch step in $Cl_2$ is used to remove any TiN remnants due to its high selectivity against the HfO below the TiN layer. The proposed model greatly simplifies simulations

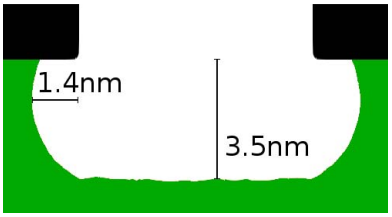


Fig. 3. Profile created by $Cl_2/CH_4$ etching for 4s with ion, Cl and $CH_4$ fluxes of $1.0x10^{15}cm^{-2}s^{-1}$, $5.0x10^{15}cm^{-2}s^{-1}$ and $2.8x10^{16}$ $cm^{-2}s^{-1}$, respectively. In a gate stack, the TiN layer is roughly 3.5nm thick, which is why this etch depth was chosen.

for uniform etch chemistries, as there is only one surface coverage to track, that of the etchant. The underlying HfSiO layer is then etched in $BCl_3/Cl_2$, which is also highly isotropic without damaging the underlying material, due to its near-infinite selectivity towards the Si substrate [10].

## IV. Results

A full gate stack etching sequence was simulated to show that the proposed model enables accurate modelling, not only of each process individually, but also of the interplay between all involved processes and to include the effects of one etch step on the subsequent ones. Especially the different passivation layers and their combined influence on the final geometry of the gate stack is of particular interest.

### A. Poly-Si Main Etch

As described earlier, the gate stack etch process for the 14nm node starts with Poly-Si etching in a $SF_6$ type plasma etch chemistry. The profile after this etch step is shown in Fig. 4, highlighting the directional characteristic of this chemistry. The slant resulting from the deposition of polymer (blue) layers on the sidewallsof the Poly-Si (pink) can be seen clearly. Furthermore, the thickness of the polymer layer decreases towards the etched substrate, while it completely covers the surface in already etched regions as expected.

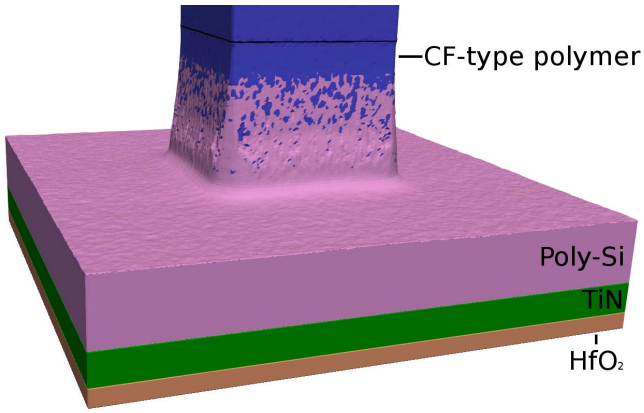


Fig. 4. Gate geometry after $SF_6$ type etching for 60s with ion, etchant and polymer fluxes of: $1.5x10^{15}cm^{-2}s^{-1}$, $1.3x10^{16}cm^{-2}s^{-1}$, $4.5x10^{15}$ $cm^{-2}s^{-1}$, respectively. The black horizontal line indicates the border between the mask and the Poly-Si (pink) beneath the polymer (blue).

### B. Poly-Si Over Etch

In order not to damage TiN underneath the Poly-Si, a more selective chemistry than in the main etch step is used. This results in more slanted profiles due to the strong deposition of polymer during etching with $HBr/O_2$ plasma chemistries, which creates several nanometres thick passivation layers, as depicted in Fig. 5.

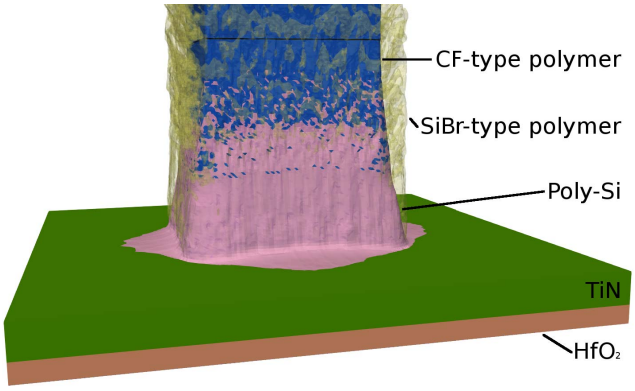


Fig. 5. Exposed TiN (green) surface after the Poly-Si (pink) over etch with ion, O and Br fluxes of $1.0x10^{16}cm^{-2}s^{-1}$, $2.0x10^{16}cm^{-2}s^{-1}$ and $1.0x10^{16}$ $cm^{-2}s^{-1}$, respectively. A new passivation layer (transparent yellow) formed on top of the already existing polymer. The black line indicates the bottom of the mask underneath the passivation layer.

### C. TiN Main Etch, TiN Over Etch and $HfO_2$ Etch

As described above, the $Cl_2/CH_4$ chemistry used in this step is not as directional as those of the Si etch step, but it is selective against Si, so it will not etch the exposed parts of the Si sidewall. The remaining TiN is removed in an isotropic $Cl_2$ etch step to leave a clear surface for the last etch step, as can be seen in Fig. 6. The TiN etch steps are then followed by $HfO_2$ etching, which is isotropic, highly selective and can even thicken the existing passivation layers chemically, [3] as shown in Fig. 7.

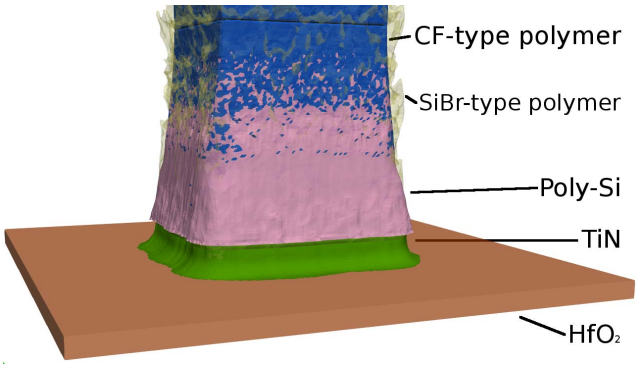


Fig. 6. Gate stack geometry after both TiN etch steps. The TiN Main Etch was carried out for 4s with ion, Cl and $CH_4$ fluxes of $1.0x10^{15}cm^{-2}s^{-1}$, $5.0x10^{15}cm^{-2}s^{-1}$ and $2.8x10^{16}$ $cm^{-2}s^{-1}$, respectively. The TiN Over Etch was then simulated using a Cl flux of $5x10^{16}$ $cm^{-2}s^{-1}$, leaving the $HfO_2$ surface exposed.

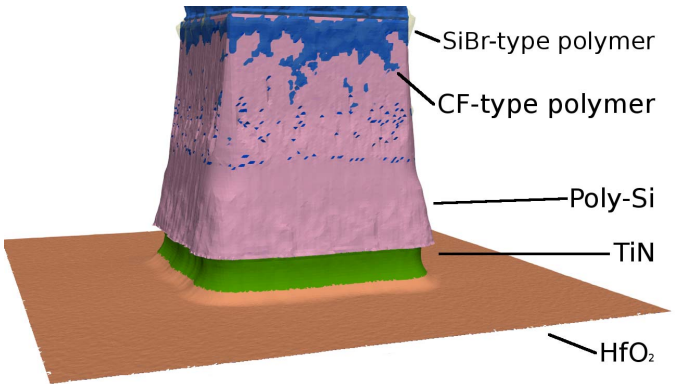


Fig. 7. After the final etch step, the profile of the gate has several features due to the varying characteristics of the etch chemistries, such as a tapered Poly-Si profile, a concave TiN profile due to under-etching and the removal of the earlier deposited polymers, leaving only remnants of some.

## V. Conclusion

A unified feature scale model has been implemented into a levelset powered process simulator, to enable the simulation of complex etch sequences used in the etching of transistor gate stacks. Each of the involved chemistries could be represented accurately within this single model, using different parameters to mimic their respective behaviour. The properties of the simulated chemistries are in good agreement with theory and the profile obtained from the simulation of a full gate stack etching process shows good agreement to experimental results. The final profile, shown in Fig. 7, highlights the interplay of different passivating effects during Poly-Si etching with more uniform and selective chemistries in subsequent etch steps. This creates a complex geometry with several typical features such as tapered profiles combined with under-etches on the sidewalls, which matches the characteristics observed in experimentherefore, we can be confident in the results provided by the simulator being physical within the mentioned limitations, even for complex etching processes.

## Acknowledgment

The research leading to these results has received funding from the European Unions Horizon 2020 research and innovation programme under grant agreement No 688101 SUPERAID7.

## References

[1] International Technology Roadmap for Semiconductors, 2015.
[2] O. Luere *et al.*, *J. Vac. Sci. Technol., B*, **29**(1), p. 011028(10), 2011.
[3] O. R. Bengoetxea, Ph.D. dissertation, Université Grenoble Alpes, 2016.
[4] ViennaTS. [Online]. Available: https://github.com/viennats/viennats-dev
[5] A. Magna and G. Garozzo, *J. Electrochem. Soc.*, **150**(10), pp. F178–F185, 2011.
[6] B. E. Thompson and H. H. Sawin, *J. Electrochem. Soc.*, **133**(9), pp. 1887–1895, 1986.
[7] R. J. Belen *et al.*, *J. Vac. Sci. Technol., A*, **23**(5), pp. 1430–1439, 2005.
[8] L. Desvoivres *et al.*, *J. Vac. Sci. Technol., B*, **19**(2), pp. 420–426, 2001.
[9] N. M. Muthukrishnan and K. Amberiadis, *J. Electrochem. Soc.*, **144**(5), pp. 1780–1784, 1997.
[10] E. Sungauer *et al.*, *J. Vac. Sci. Technol., B*, **25**(5), pp. 1640–1646, 2007.